Coordinated Adaptive Robust Contour Tracking of Linear-Motor-Driven Tables in Task Space [1]

Li Xu Bin Yao [+]

School of Mechanical Engineering
Purdue University
West Lafayette, IN 47907, USA
[+] Email: byao@ecn.purdue.edu

Abstract

In order to improve the overall contouring performance, it appears that it is no longer possible to neglect dynamic coupling phenomena that occur during contour tracking, especially for linear motor systems which often move at high speed. This paper studies the high performance contour tracking control of linear-motor-driven tables. The table dynamics is first transformed into a task coordinate frame. A discontinuous projection based adaptive robust controller (ARC) which explicitly takes into account the dynamic coupling effect is constructed to improve the contouring performance under both parametric uncertainties and uncertain nonlinearities. A desired compensation ARC scheme is also presented, in which the regressor is calculated using desired contour information only. Both schemes are implemented and compared on a linear-motor-driven X-Y table.

1 Introduction

A great deal of effort has been devoted to solving independent axial control problems of linear-motor-driven systems [1]–[5]. In these designs, each axis of motion is separately driven and the servo controller of one axis receives no information regarding the other axes. This results in a collection of decoupled single input and single output (SISO) systems. Decoupled design may be preferable if the disturbance in one axis should not affect the performance of other axes. For contouring applications, however, decoupling is sometimes damaging to the overall performance objective [6].

A more appropriate approach to address the contour tracking problem is to introduce coupling actions in the servo controllers so that the motion axes are "coordinated" to track the desired contour. In [7], Koren proposed the cross-coupled strategy. The control of multiple axes is treated as a single control unit and the control of one axial servomechanism is affected by other axial servomechanisms involved in the motion. In [8], Srinivasan and Fosdick proposed a multivariable analysis approach to motion coordination under the assumption that the desired contour is a combination of piecewise linear segments. Recently, Koren and Lo [9] introduced a variable-gain cross-coupled controller for a general class of contours. One limitation of these approaches is that they cannot effectively address the dynamic coupling phenomena (e.g. Coriolis force) occur when tracking curved contours, since these designs are based on the traditional linear time-invariant theories. In [6], Chiu and Tomizuka formulated the contour tracking problem in a "desired" task coordinate frame. However, the proposed task coordinate frame was based on the desired contour which is only an approximation of the actual task coordinate frame.

In this paper, the idea of adaptive robust control (ARC) of robot manipulators in task space [10] is utilized to solve the contour tracking problem of a linear-motor-driven table. The table dynamics is first transformed into a task coordinate frame. A discontinuous projection based adaptive robust controller [11] is then constructed to improve the contouring performance. As pointed out in [12], however, this algorithm may have several potential implementation problems since the regressor depends on the states of the system. As a remedy, a desired compensation ARC [12] in which the regressor is calculated based on the desired contour information only is then developed. Finally, comparative experimental results are presented to show the advantages and the drawbacks of each method.

2 Problem Formulation

The linear-motor-driven X-Y positioning table is assumed to have the following dynamics [5]:

$$\mathbf{M}\ddot{\mathbf{q}} + \mathbf{B}\dot{\mathbf{q}} + \mathbf{F}(\dot{\mathbf{q}}) = \mathbf{u} + \mathbf{d}, \tag{1}$$

where $\mathbf{q}$, $\dot{\mathbf{q}}$ and $\ddot{\mathbf{q}}$ are the 2×1 vectors of the axis position, velocity and acceleration, respectively; $\mathbf{u}$ is the 2×1 vector of control input, and $\mathbf{d}$ is the 2×1 vector of unknown nonlinear functions due to external disturbances or modeling errors (e.g., force ripple); $\mathbf{M}$ and $\mathbf{B}$ are the 2×2 diagonal inertia and damping matrices, respectively; $\mathbf{F}(\dot{\mathbf{q}})$ is the 2×1 vector of nonlinear friction, i.e., $\mathbf{F}(\dot{\mathbf{q}}) = [F_1(\dot{q}_1),\ F_2(\dot{q}_2)]^T$, and $F_i(\dot{q}_i)$ is

[1] The work is supported in part by the National Science Foundation under the CAREER grant CMS-9734345 and in part by a grant from Purdue Research Foundation

often modeled as [13]

$$F_i(\dot{q}_i) = -[f_{ci} + (f_{si} - f_{ci})e^{-|\dot{q}_i/\dot{q}_{si}|^{\xi_i}}]\mathrm{sgn}(\dot{q}_i), \quad i = 1,2, \tag{2}$$

where f_{si} is the level of static friction, f_{ci} is the level of Coulomb friction, and $\dot{q}_{si}$ and ξ_i are empirical parameters used to describe the Stribeck effect. It is seen that the friction model (2) is discontinuous at $\dot{q}_i = 0$. Thus one cannot use this model for friction compensation. To by-pass this technical difficulty, a simple smooth friction model will be used to approximate the actual friction model (2) for model compensation. The model used in this paper is given by $\bar{\mathbf{F}}(\dot{\mathbf{q}}) = \mathbf{A}\mathbf{S_f}(\dot{\mathbf{q}})$, where $\mathbf{A}$ is the 2×2 diagonal friction coefficient matrix, and $\mathbf{S_f}(\cdot)$ is a vector-valued smooth function i.e.,$\mathbf{S_f}(\dot{\mathbf{q}}) = [S_f(\dot{q}_1),\ S_f(\dot{q}_2)]^T$. Define the approximation error as $\tilde{\mathbf{F}} = \bar{\mathbf{F}} - \mathbf{F}$. Then equation (1) can be written as

$$\mathbf{M}\ddot{\mathbf{q}} + \mathbf{B}\dot{\mathbf{q}} + \mathbf{A}\mathbf{S_f}(\dot{\mathbf{q}}) = \mathbf{u} + \mathbf{d_n} + \tilde{\mathbf{d}}, \tag{3}$$

where $\mathbf{d_n}$ is the nominal value of $\mathbf{d_l} \triangleq \mathbf{d} + \tilde{\mathbf{F}}$, and $\tilde{\mathbf{d}} = \mathbf{d_l} - \mathbf{d_n}$. Based on the design model (3), in the following, we will formulate the contour tracking problem in task space. Suppose a desired contour in $\mathbb{R}^2$ is given by $\mathbf{q_d}(t) = [q_{1d}(t), q_{2d}(t)]^T$. Then, the curve $\mathbf{q_d}(t)$ can be represented implicitly by the function $f(q_{1d}(t), q_{2d}(t)) = 0$, and the curve length is given by

$$g(q_{1d}(t), q_{2d}(t)) = \int_0^t \|\frac{d}{d\tau}\mathbf{q_d}(\tau)\|\mathrm{d}\tau. \tag{4}$$

A task coordinate system $\mathbf{r} \in \mathbb{R}^2$ can be defined as

$$\mathbf{r} = \mathbf{h}(\mathbf{q}) = \begin{bmatrix} f(\mathbf{q}) \\ g(\mathbf{q}) \end{bmatrix} = \begin{bmatrix} f(q_1(t), q_2(t)) \\ g(q_1(t), q_2(t)) \end{bmatrix}. \tag{5}$$

Differentiating (5) twice yields

$$\dot{\mathbf{r}} = \mathbf{J}\dot{\mathbf{q}}, \quad \ddot{\mathbf{r}} = \mathbf{J}\ddot{\mathbf{q}} + \dot{\mathbf{J}}\dot{\mathbf{q}}, \tag{6}$$

where $\mathbf{J}(\mathbf{q}) = \partial\mathbf{h}/\partial\mathbf{q}$ is the Jacobian matrix. It is assumed that in the finite workspace $\mathbf{q} \in \Omega_q$, the mapping $\mathbf{h}(\mathbf{q}) : \Omega_q \to \Omega_r$ is one-to-one and the Jacobian matrix $\mathbf{J}$ is nonsingular. Using (6), (3) can be represented in the task space as

$$\mathbf{M_t}(\mathbf{r})\ddot{\mathbf{r}} + \mathbf{B_t}(\mathbf{r})\dot{\mathbf{r}} + \mathbf{C_t}(\mathbf{r},\dot{\mathbf{r}})\dot{\mathbf{r}} + \mathbf{A_t}(\mathbf{r})\mathbf{S_f}(\dot{\mathbf{q}}) = \mathbf{u_t} + \mathbf{d_t}(\mathbf{r}) + \tilde{\Delta}, \tag{7}$$

where

$$\begin{array}{l} \mathbf{M_t} = \mathbf{J^{-T}M J^{-1}},\ \mathbf{B_t} = \mathbf{J^{-T}B J^{-1}},\ \mathbf{C_t} = -\mathbf{J^{-T}M J^{-1}\dot{J} J^{-1}}, \\ \mathbf{A_t} = \mathbf{J^{-T}A},\ \mathbf{d_t} = \mathbf{J^{-T}d_n},\ \mathbf{u_t} = \mathbf{J^{-T}u},\ \tilde{\Delta} = \mathbf{J^{-T}}\tilde{\mathbf{d}}. \end{array} \tag{8}$$

It is well known that equation (7) has several properties [10]:

P 1 *In the finite work space Ω_q, $\mathbf{M_t}(\mathbf{r})$ is a symmetric positive definite (s.p.d.) matrix with*

$$\mu_1\mathbf{I} \le \mathbf{M_t}(\mathbf{r}) \le \mu_2\mathbf{I}, \quad \forall\mathbf{q} \in \Omega_q, \tag{9}$$

where μ_1 and μ_2 are two positive scalars.

P 2 *Given the definitions in (8), the matrix $\mathbf{N}(\mathbf{r},\dot{\mathbf{r}}) = \dot{\mathbf{M}}_\mathbf{t}(\mathbf{r}) - 2\mathbf{C_t}(\mathbf{r},\dot{\mathbf{r}})$ is a skew-symmetric matrix.*

P 3 *The task space dynamics (7) is linear in terms of a set of parameters, such as inertia $\mathbf{M}$, damping coefficient $\mathbf{B}$, friction coefficient $\mathbf{A}$ and nominal disturbance $\mathbf{d_n}$, i.e.,*

$$\mathbf{M_t}\ddot{\mathbf{r}} + \mathbf{B_t}\dot{\mathbf{r}} + \mathbf{C_t}(\mathbf{r},\dot{\mathbf{r}})\dot{\mathbf{r}} + \mathbf{A_t}(\mathbf{r})\mathbf{S_f}(\dot{\mathbf{q}}) - \mathbf{d_t} = -\psi(\mathbf{r},\dot{\mathbf{r}},\dot{\mathbf{r}},\ddot{\mathbf{r}})\theta, \tag{10}$$

*where ψ is a 2×8 matrix of known functions, known as the **regressor**, and θ is an 8-dimensional vector of unknown parameters defined as $\theta = [\theta_1,\cdots,\theta_8]^T = [M_1, M_2, B_1, B_2, A_1, A_2, d_{n1}, d_{n2}]^T$.*

In general, the parameter θ cannot be known exactly. For example, the payload of the X-Y table depends on tasks. However, the extent of parametric uncertainties can be predicted. Therefore, the following practical assumption is made. (For simplicity, the following notations are used: $\bullet_i$ for the i-th component of the vector $\bullet$, $\bullet_{\min}$ for the minimum value of $\bullet$, and $\bullet_{\max}$ for the maximum value of $\bullet$. The operation $<$ for two vectors is performed in terms of the corresponding elements of the vectors.)

Assumption 1 *The extent of the parametric uncertainties and uncertain nonlinearities is known, i.e.,*

$$\theta \in \Omega_\theta \triangleq \{\ \theta :\ \theta_{\min} \le \theta \le \theta_{\max}\ \}, \tag{11}$$

$$\tilde{\Delta} \in \Omega_\Delta \triangleq \{\tilde{\Delta} :\ \|\tilde{\Delta}\| \le \delta_\Delta\ \}, \tag{12}$$

where $\theta_{\min} = [\theta_{1\min},\ \cdots,\ \theta_{8\min}]^T$, $\theta_{\max} = [\theta_{1\max},\ \cdots,\ \theta_{8\max}]^T$, and δ_Δ are known. ◇

The control objective is to synthesize a control input $\mathbf{u_t}$ such that $\mathbf{r}$ tracks a desired contour $\mathbf{r_d}(t)$ which is assumed to be third-order differentiable.

3 Discontinuous Projection

Let $\hat{\theta}$ denote the estimate of θ and $\tilde{\theta}$ the estimation error (i.e., $\tilde{\theta} = \hat{\theta} - \theta$). In view of (11), the following adaptation law with discontinuous projection modification can be used

$$\dot{\hat{\theta}} = \mathrm{Proj}_{\hat{\theta}}(\Gamma\tau), \tag{13}$$

where $\Gamma > 0$ is a diagonal matrix, τ is an adaptation function to be synthesized later. The projection mapping $\mathrm{Proj}_{\hat{\theta}}(\bullet) = [\mathrm{Proj}_{\hat{\theta}_1}(\bullet_1),\cdots,\mathrm{Proj}_{\hat{\theta}_p}(\bullet_p)]^T$ is defined in [14, 11] as

$$\mathrm{Proj}_{\hat{\theta}_i}(\bullet_i) = \begin{cases} 0 & \text{if } \hat{\theta}_i = \theta_{i\max} \text{ and } \bullet_i > 0 \\ 0 & \text{if } \hat{\theta}_i = \theta_{i\min} \text{ and } \bullet_i < 0 \\ \bullet_i & \text{otherwise} \end{cases} \tag{14}$$

It can be shown [15] that for any adaptation function τ, the projection mapping used in (14) guarantees

$$\begin{array}{ll} \mathbf{P4} & \hat{\theta} \in \Omega_\theta \triangleq \{\hat{\theta} : \theta_{\min} \le \hat{\theta} \le \theta_{\max}\} \\ \mathbf{P5} & \tilde{\theta}^\mathbf{T}\left(\Gamma^{-1}\mathrm{Proj}_{\hat{\theta}}(\Gamma\tau) - \tau\right) \le 0, \quad \forall\tau \end{array} \tag{15}$$

4 Adaptive Robust Control (ARC) Law Synthesis

Define a switching-function-like quantity as

$$\mathbf{s} = \dot{\mathbf{e}} + \Lambda\mathbf{e} = \dot{\mathbf{r}} - \dot{\mathbf{r}}_\mathbf{eq}, \quad \dot{\mathbf{r}}_\mathbf{eq} \triangleq \dot{\mathbf{r}}_\mathbf{d} - \Lambda\mathbf{e}, \tag{16}$$

where $\mathbf{e} = \mathbf{r}(t) - \mathbf{r_d}(t)$ is the output tracking error, and $\Lambda > 0$ is a diagonal matrix. Define a positive semi-definite (p.s.d.) function

$$V(t) = \frac{1}{2}\mathbf{s^T M_t}(\mathbf{r})\mathbf{s}. \tag{17}$$

Differentiating V yields

$$\dot{V}(t) = \mathbf{s^T}\left[\mathbf{u_t} - \mathbf{M_t}\ddot{\mathbf{r}}_\mathbf{eq} - \mathbf{B_t}\dot{\mathbf{r}} - \mathbf{C_t}\dot{\mathbf{r}}_\mathbf{eq} - \mathbf{A_t}\mathbf{S_f}(\dot{\mathbf{q}}) + \mathbf{d_t} + \tilde{\Delta}\right], \tag{18}$$

where $\ddot{\mathbf{r}}_\mathbf{eq} \triangleq \ddot{\mathbf{r}}_\mathbf{d} - \Lambda\dot{\mathbf{e}}$, and P2 is used to eliminate the term $\frac{1}{2}\mathbf{s^T}\dot{\mathbf{M}}_\mathbf{t}(\mathbf{r})\mathbf{s}$. Furthermore, since it follows from P3 that

$$\mathbf{M_t}\ddot{\mathbf{r}}_\mathbf{eq} + \mathbf{B_t}\dot{\mathbf{r}} + \mathbf{C_t}\dot{\mathbf{r}}_\mathbf{eq} + \mathbf{A_t}\mathbf{S_f}(\dot{\mathbf{q}}) - \mathbf{d_t} = -\psi(\mathbf{r},\dot{\mathbf{r}},\dot{\mathbf{r}}_\mathbf{eq},\ddot{\mathbf{r}}_\mathbf{eq})\theta, \tag{19}$$

equation (18) can be rewritten as

$$\dot{V}(t) = \mathbf{s^T}\Big[\mathbf{u_t} + \psi(\mathbf{r},\dot{\mathbf{r}},\dot{\mathbf{r}}_{\mathbf{eq}},\ddot{\mathbf{r}}_{\mathbf{eq}})\theta + \tilde{\Delta}\Big]. \tag{20}$$

Noting the structure of (20), the following ARC law is proposed:

$$\mathbf{u_t} = \mathbf{u_a} + \mathbf{u_s}, \quad \mathbf{u_a} = -\psi(\mathbf{r},\dot{\mathbf{r}},\dot{\mathbf{r}}_{\mathbf{eq}},\ddot{\mathbf{r}}_{\mathbf{eq}})\hat{\theta}, \tag{21}$$

where $\mathbf{u_a}$ is the adjustable model compensation needed for achieving perfect tracking, and $\mathbf{u_s}$ is a robust control law to be synthesized later. Substituting (21) into (20), and then simplifying the resulting expression lead to

$$\dot{V} = \mathbf{s^T}\Big[\mathbf{u_s} - \psi(\mathbf{r},\dot{\mathbf{r}},\dot{\mathbf{r}}_{\mathbf{eq}},\ddot{\mathbf{r}}_{\mathbf{eq}})\tilde{\theta} + \tilde{\Delta}\Big]. \tag{22}$$

The robust control function $\mathbf{u_s}$ consists of two terms:

$$\mathbf{u_s} = \mathbf{u_{s1}} + \mathbf{u_{s2}}, \quad \mathbf{u_{s1}} = -\mathbf{K}\mathbf{s}, \tag{23}$$

where $\mathbf{u_{s1}}$ is used to stabilize the nominal system, and it is a simple proportional feedback with $\mathbf{K}$ being a symmetric positive definite matrix in this case, and $\mathbf{u_{s2}}$ is a robust feedback used to attenuate the effect of model uncertainties. Noting Assumption 1 and P4 of (15), there exists a $\mathbf{u_{s2}}$ such that the following two conditions are satisfied

$$\begin{array}{ll} \text{i} & \mathbf{s^T}\{\mathbf{u_{s2}} - \psi(\mathbf{r},\dot{\mathbf{r}},\dot{\mathbf{r}}_{\mathbf{eq}},\ddot{\mathbf{r}}_{\mathbf{eq}})\tilde{\theta} + \tilde{\Delta}\} \le \varepsilon \\ \text{ii} & \mathbf{s^T}\mathbf{u_{s2}} \le 0 \end{array} \tag{24}$$

where ε is a design parameter that can be arbitrarily small. One smooth example of $\mathbf{u_{s2}}$ satisfying (24) is given by $\mathbf{u_{s2}} = -\frac{1}{4\varepsilon}h^2\mathbf{s}$, where h is a smooth function satisfying $h \ge \|\theta_{\mathbf{M}}\|\|\psi(\mathbf{r},\dot{\mathbf{r}},\dot{\mathbf{r}}_{\mathbf{eq}},\ddot{\mathbf{r}}_{\mathbf{eq}})\| + \delta_\Delta$, and $\theta_{\mathbf{M}} = \theta_{\max} - \theta_{\min}$.

Theorem 1 *Suppose the adaptation function in (13) is chosen as*

$$\tau = \psi^{\mathbf{T}}(\mathbf{r},\dot{\mathbf{r}},\dot{\mathbf{r}}_{\mathbf{eq}},\ddot{\mathbf{r}}_{\mathbf{eq}})\mathbf{s}. \tag{25}$$

Then, the ARC control law (21) guarantees that:

A. *In general, all signals are bounded. Furthermore, the positive semi-definite function $V(t)$ defined by (17) is bounded above by*

$$V(t) \le \exp(-\lambda t)V(0) + \frac{\varepsilon}{\lambda}\Big[1 - \exp(-\lambda t)\Big], \tag{26}$$

where $\lambda = 2\sigma_{\min}(\mathbf{K})/\mu_2$, and $\sigma_{\min}(\cdot)$ denotes the minimum eignvalue of a matrix. Note that $\sigma_{\min}(\mathbf{K})$ is real and positive since $\mathbf{K}$ is symmetric positive definite.

B. *Suppose there exist parametric uncertainties only after a finite time t_0, i.e., $\tilde{\Delta} = \mathbf{0}$, $\forall t \ge t_0$. Then, in addition to result **A**, zero final tracking error is also achieved, i.e, $\mathbf{e} \longrightarrow 0$ and $\mathbf{s} \longrightarrow 0$ as $t \longrightarrow \infty$.*

Proof: The proof of Theorem 1 is similar to the proof of Theorem 2 in the following, and therefore it is omitted.

5 Desired Compensation ARC (DCARC)

In the ARC design presented in Section 4, the regressor $\psi(\mathbf{r},\dot{\mathbf{r}},\dot{\mathbf{r}}_{\mathbf{eq}},\ddot{\mathbf{r}}_{\mathbf{eq}})$ in the model compensation $\mathbf{u_a}$ (21) and adaptation function τ (25) depends on states $\mathbf{r}$ and $\dot{\mathbf{r}}$. Such an adaptation structure may have several potential implementation problems [12]. First, the effect of measurement noise may be severe, and a slow adaptation rate may have to be used, which in turn reduces the effect of parameter adaptation. Secondly, there may exist certain interactions between the model compensation $\mathbf{u_a}$ and the robust control $\mathbf{u_s}$. This may complicate the controller gain tuning process in implementation. In [16], Sadegh and Horowitz proposed a desired compensation adaptation law, in which the regressor is calculated by desired trajectory information only. This idea was then incorporated in the ARC design in [12]. In the following, the desired compensation ARC is applied on the linear-motor-driven X-Y table.

The proposed DCARC law and adaptation function have the same form as (21) and (25), but with the regressor $\psi(\mathbf{r},\dot{\mathbf{r}},\dot{\mathbf{r}}_{\mathbf{eq}},\ddot{\mathbf{r}}_{\mathbf{eq}})$ substituted by the desired regressor $\psi_{\mathbf{d}}(\mathbf{r_d},\dot{\mathbf{r}}_{\mathbf{d}},\dot{\mathbf{r}}_{\mathbf{d}},\ddot{\mathbf{r}}_{\mathbf{d}})$:

$$\begin{array}{l} \mathbf{u_t} = \mathbf{u_a} + \mathbf{u_s}, \qquad \mathbf{u_a} = -\psi_{\mathbf{d}}(\mathbf{r_d},\dot{\mathbf{r}}_{\mathbf{d}},\dot{\mathbf{r}}_{\mathbf{d}},\ddot{\mathbf{r}}_{\mathbf{d}})\hat{\theta}, \\ \tau = \psi_{\mathbf{d}}^{\mathbf{T}}(\mathbf{r_d},\dot{\mathbf{r}}_{\mathbf{d}},\dot{\mathbf{r}}_{\mathbf{d}},\ddot{\mathbf{r}}_{\mathbf{d}})\mathbf{s}. \end{array} \tag{27}$$

Choose a positive semi-definite function

$$V(t) = \frac{1}{2}\mathbf{s^T}\mathbf{M_t}(\mathbf{r})\mathbf{s} + \frac{1}{2}\mathbf{e^T}\mathbf{K_e}\mathbf{e}, \tag{28}$$

where $\mathbf{K_e}$ is a s.p.d. matrix. Differentiating $V(t)$ and substituting (27) into the resulting expression yields

$$\dot{V}(t) = \mathbf{s^T}\Big[\mathbf{u_s} + \tilde{\psi}\theta - \psi_{\mathbf{d}}(\mathbf{r_d},\dot{\mathbf{r}}_{\mathbf{d}},\dot{\mathbf{r}}_{\mathbf{d}},\ddot{\mathbf{r}}_{\mathbf{d}})\tilde{\theta} + \tilde{\Delta}\Big] + \mathbf{e^T}\mathbf{K_e}\dot{\mathbf{e}}, \tag{29}$$

where $\tilde{\psi} = \psi(\mathbf{r},\dot{\mathbf{r}},\dot{\mathbf{r}}_{\mathbf{eq}},\ddot{\mathbf{r}}_{\mathbf{eq}}) - \psi_{\mathbf{d}}(\mathbf{r_d},\dot{\mathbf{r}}_{\mathbf{d}},\dot{\mathbf{r}}_{\mathbf{d}},\ddot{\mathbf{r}}_{\mathbf{d}})$ is the difference between the actual regression matrix and the desired regression matrix formulations. As shown in [16], $\tilde{\psi}$ can be quantified as

$$\|\tilde{\psi}\theta\| \le \zeta_1\|\mathbf{e}\| + \zeta_2\|\mathbf{e}\|^2 + \zeta_3\|\mathbf{s}\| + \zeta_4\|\mathbf{s}\|\|\mathbf{e}\|, \tag{30}$$

where ζ_1,ζ_2,ζ_3 and ζ_4 are positive bounding constants that depend on the desired contour and the physical properties of the X-Y table configuration. Similar to (23), the robust control function $\mathbf{u_s}$ consists of two terms given by:

$$\mathbf{u_s} = \mathbf{u_{s1}} + \mathbf{u_{s2}}, \quad \mathbf{u_{s1}} = -\mathbf{K}\mathbf{s} - \mathbf{K_e}\mathbf{e} - \mathbf{K_a}\|\mathbf{e}\|^2\mathbf{s}, \tag{31}$$

where the controller parameters $\mathbf{K}$, $\mathbf{K_e}$ and $\mathbf{K_a}$ are s.p.d. matrices satisfying $\sigma_{\min}(\mathbf{K_a}) \ge \zeta_2 + \zeta_4$ and the following condition

$$\mathbf{Q} = \begin{bmatrix} \sigma_{\min}(\mathbf{K_e}\Lambda) - \frac{1}{4}\zeta_2 & -\frac{1}{2}\zeta_1 \\ -\frac{1}{2}\zeta_1 & \sigma_{\min}(\mathbf{K}) - \zeta_3 - \frac{1}{4}\zeta_4 \end{bmatrix} > 0. \tag{32}$$

Specifically, it is easy to check that if

$$\sigma_{\min}(\mathbf{K_e}\Lambda) \ge \frac{1}{2}\zeta_1 + \frac{1}{4}\zeta_2, \quad \sigma_{\min}(\mathbf{K}) \ge \frac{1}{2}\zeta_1 + \zeta_3 + \frac{1}{4}\zeta_4, \tag{33}$$

the matrix $\mathbf{Q}$ defined in (32) is positive definite. The robust control term $\mathbf{u_{s2}}$ is required to satisfy the following constrains similar to (24),

$$\begin{array}{ll} \text{i} & \mathbf{s^T}\{\mathbf{u_{s2}} - \psi_{\mathbf{d}}(\mathbf{r_d},\dot{\mathbf{r}}_{\mathbf{d}},\dot{\mathbf{r}}_{\mathbf{d}},\ddot{\mathbf{r}}_{\mathbf{d}})\tilde{\theta} + \tilde{\Delta}\} \le \varepsilon \\ \text{ii} & \mathbf{s^T}\mathbf{u_{s2}} \le 0 \end{array} \tag{34}$$

One smooth example of $\mathbf{u_{s2}}$ satisfying (34) is $\mathbf{u_{s2}} = -\frac{1}{4\varepsilon}h_d^2\mathbf{s}$, where h_d is any function satisfying $h_d \ge \|\theta_{\mathbf{M}}\|\|\psi_{\mathbf{d}}(\mathbf{r_d},\dot{\mathbf{r}}_{\mathbf{d}},\dot{\mathbf{r}}_{\mathbf{d}},\ddot{\mathbf{r}}_{\mathbf{d}})\| + \delta_\Delta$.

Theorem 2 *The desired compensation ARC law (27) guarantees that*

A. *In general, all signals are bounded. Furthermore, the positive semi-definite function $V(t)$ defined by (28) is bounded above by*

$$V(t) \leq \exp(-\lambda t)V(0) + \frac{\varepsilon}{\lambda}\Big[1-\exp(-\lambda t)\Big], \tag{35}$$

where $\lambda = \frac{2\sigma_{\min}(\mathbf{Q})}{\max[\mu_2,\, \sigma_{\max}(\mathbf{K_e})]}$, and $\sigma_{\max}(\cdot)$ denotes the maximum eignvalue of a matrix.

B. *Suppose there exist parametric uncertainties only after a finite time t_0, i.e., $\tilde{\Delta} = \mathbf{0}$, $\forall t \geq t_0$. Then, in addition to result **A**, zero final tracking error is also achieved, i.e, $\mathbf{e} \longrightarrow 0$ and $\mathbf{s} \longrightarrow 0$ as $t \longrightarrow \infty$.*

Proof: Substituting $\dot{\mathbf{e}} = \mathbf{s} - \Lambda\mathbf{e}$ into (29), one can place an upper bound on $\dot{V}$ in the following manner

$$\begin{aligned}\dot{V}(t) \leq\ & \mathbf{s^T}\Big[\mathbf{u_s} - \psi_{\mathbf{d}}(\mathbf{r_d}, \dot{\mathbf{r}}_{\mathbf{d}}, \dot{\mathbf{r}}_{\mathbf{d}}, \ddot{\mathbf{r}}_{\mathbf{d}})\tilde{\theta} + \tilde{\delta}\Big] + \|\mathbf{s}\|\|\tilde{\psi}\theta\| \\ & + \mathbf{e^T K_e s} - \mathbf{e^T K_e \Lambda e}\end{aligned} \tag{36}$$

Substituting (30), (31) and condition i of (34) into (36) yields

$$\begin{aligned}\dot{V}(t) \leq & -\mathbf{s^T K s} - \|\mathbf{e}\|^2\mathbf{s^T K_a s} + \|\mathbf{s}\|\|\tilde{\psi}\theta\| - \mathbf{e^T K_e \Lambda e} + \varepsilon \\ \leq & -\sigma_{\min}(\mathbf{K})\|\mathbf{s}\|^2 - \sigma_{\min}(\mathbf{K_a})\|\mathbf{e}\|^2\|\mathbf{s}\|^2 + \zeta_1\|\mathbf{s}\|\|\mathbf{e}\| + \varepsilon \\ & + \zeta_2\|\mathbf{s}\|\|\mathbf{e}\|^2 + \zeta_3\|\mathbf{s}\|^2 + \zeta_4\|\mathbf{s}\|^2\|\mathbf{e}\| - \sigma_{\min}(\mathbf{K_e}\Lambda)\|\mathbf{e}\|^2\end{aligned} \tag{37}$$

By using completion of square, (37) can be written as

$$\begin{aligned}\dot{V}(t) \leq & -\sigma_{\min}(\mathbf{K})\|\mathbf{s}\|^2 - \sigma_{\min}(\mathbf{K_a})\|\mathbf{e}\|^2\|\mathbf{s}\|^2 + \zeta_1\|\mathbf{s}\|\|\mathbf{e}\| \\ & -\zeta_2\|\mathbf{e}\|^2(\tfrac{1}{2} - \|\mathbf{s}\|)^2 + \tfrac{1}{4}\zeta_2\|\mathbf{e}\|^2 + \zeta_2\|\mathbf{e}\|^2\|\mathbf{s}\|^2 + \zeta_3\|\mathbf{s}\|^2 \\ & -\zeta_4\|\mathbf{s}\|^2(\tfrac{1}{2} - \|\mathbf{e}\|)^2 + \tfrac{1}{4}\zeta_4\|\mathbf{s}\|^2 + \zeta_4\|\mathbf{e}\|^2\|\mathbf{s}\|^2 \\ & -\sigma_{\min}(\mathbf{K_e}\Lambda)\|\mathbf{e}\|^2 + \varepsilon\end{aligned} \tag{38}$$

After collecting common terms in (38), it can be rewritten as

$$\begin{aligned}\dot{V}(t) \leq\ & \zeta_1\|\mathbf{s}\|\|\mathbf{e}\| - \zeta_2\|\mathbf{e}\|^2(\tfrac{1}{2} - \|\mathbf{s}\|)^2 - \zeta_4\|\mathbf{s}\|^2(\tfrac{1}{2} - \|\mathbf{e}\|)^2 \\ & -[\sigma_{\min}(\mathbf{K}) - \zeta_3 - \tfrac{1}{4}\zeta_4]\|\mathbf{s}\|^2 - [\sigma_{\min}(\mathbf{K_a}) - \zeta_2 - \zeta_4] \\ & \cdot\|\mathbf{e}\|^2\|\mathbf{s}\|^2 - [\sigma_{\min}(\mathbf{K_e}\Lambda) - \tfrac{1}{4}\zeta_2]\|\mathbf{e}\|^2 + \varepsilon\end{aligned} \tag{39}$$

Suppose the control gain matrix $\mathbf{K_a}$ is large enough such that $\sigma_{\min}(\mathbf{K_a}) \geq \zeta_2 + \zeta_4$. Then, (39) becomes

$$\begin{aligned}\dot{V}(t) \leq & -[\sigma_{\min}(\mathbf{K}) - \zeta_3 - \tfrac{1}{4}\zeta_4]\|\mathbf{s}\|^2 - [\sigma_{\min}(\mathbf{K_e}\Lambda) - \tfrac{1}{4}\zeta_2]\|\mathbf{e}\|^2 \\ & + \zeta_1\|\mathbf{s}\|\|\mathbf{e}\| + \varepsilon,\end{aligned} \tag{40}$$

which can be put into a matrix form

$$\dot{V}(t) \leq -\mathbf{x^T Q x} + \varepsilon \leq \lambda V + \varepsilon, \tag{41}$$

where $\mathbf{x^T} = [\ \|\mathbf{e}\|\ \|\mathbf{s}\|\ ]$. Inequality (41) leads to (35) and result **A** of Theorem 2 is proved. Now consider the situation in **B** of Theorem 2, i.e., $\tilde{\Delta} = \mathbf{0}$, $\forall t \geq t_0$. Choose a positive definite function V_θ as

$$V_\theta(t) = V(t) + \frac{1}{2}\tilde{\theta}^T\Gamma^{-1}\tilde{\theta}. \tag{42}$$

From (41), condition ii of (34) and P2 of (15), it follows that

$$\begin{aligned}\dot{V}_\theta(t) \leq\ & -\mathbf{x^T Q x} - \mathbf{s^T}\psi_{\mathbf{d}}(\mathbf{r_d}, \dot{\mathbf{r}}_{\mathbf{d}}, \dot{\mathbf{r}}_{\mathbf{d}}, \ddot{\mathbf{r}}_{\mathbf{d}})\tilde{\theta} + \tilde{\theta}^T\Gamma^{-1}\dot{\hat{\theta}} \\ =\ & -\mathbf{x^T Q x} + \tilde{\theta}^{\mathbf{T}}\Big[\Gamma^{-1}\dot{\hat{\theta}} - \psi_{\mathbf{d}}^{\mathbf{T}}(\mathbf{r_d}, \dot{\mathbf{r}}_{\mathbf{d}}, \dot{\mathbf{r}}_{\mathbf{d}}, \ddot{\mathbf{r}}_{\mathbf{d}})\mathbf{s}\Big] \\ \leq\ & -\mathbf{x^T Q x}\end{aligned} \tag{43}$$

This shows that $\mathbf{x} \in L_2 \cap L_\infty$. It is easy to check that $\dot{\mathbf{x}}$ is bounded. So, $\mathbf{x}$ is uniformly continuous. By Barbalat's lemma, $\mathbf{x} \longrightarrow 0$ as $t \longrightarrow \infty$, which implies result **B** of Theorem 2. □

6 Comparative Experiments

6.1 Experimental Setup

To test the proposed nonlinear ARC strategies, an X-Y positioning table is set up as a test-bed. As shown in Figure 1, the two axes of the X-Y table are mounted orthogonally on a horizontal plane with the Y-axis on top of the X-axis. The position sensors of the table are two linear encoders with a resolution of 1 μm after quadrature. The velocity signal is obtained by the difference of two consecutive position measurements. Standard least-square identification is performed

Figure 1: Experimental Setup

to obtain the parameters of the table. The nominal values of $\mathbf{M}$ is $\mathbf{diag}[0.14,\ 0.027]$. To test the learning capability of the proposed ARC algorithms, a 9.1kg load is mounted on the table in experiments and the identified values of the parameters are (assume that the nominal disturbance is zero):

$$\theta = [0.21,\ 0.10,\ 0.25,\ 0.273,\ 0.06,\ 0.09,\ 0,\ 0]^T. \tag{44}$$

The bounds of the parameter variations are chosen as:

$$\begin{aligned}\theta_{\min} &= [0.10,\ 0.02,\ 0.20,\ 0.24,\ 0.05,\ 0.08,\ -1,\ -1]^T, \\ \theta_{\max} &= [0.25,\ 0.12,\ 0.35,\ 0.35,\ 0.09,\ 0.12,\ \ 1,\ \ 1]^T.\end{aligned}$$

6.2 Performance Index

As in [5], the following performance indexes will be used to measure the quality of each control algorithm:

- $\|f\|_{rms} = (\frac{1}{T}\int_0^T |f|^2 \mathrm{d}t)^{1/2}$, the *rms value* of the contouring error, is used to measure *average contouring performance*, where T represents the total running time;
- $f_M = \max_t\{|f|\}$, the maximum absolute value of the contouring error, is used to measure *transient performance*;
- $\|u_i\|_{rms} = (\frac{1}{T}\int_0^T |u_i|^2 \mathrm{d}t)^{1/2}$, the average control input of each axis, is used to evaluate the amount of *control effort*;
- $c_u = \sum_{i=1}^2 \frac{\|\Delta u_i\|_{rms}}{\|u_i\|_{rms}}$, the sum of the normalized control variations of each axis, is used to measure the *degree of control chattering*, where $\|\Delta u_i\|_{rms} = \sqrt{\frac{1}{N}\sum_{j=1}^N |u_i(j\Delta T) - u_i((j-1)\Delta T)|^2}$ is the average of control input increments of each axis.

6.3 Comparative Experimental Results

The control system is implemented using a dSPACE DS1103 controller board. The controller executes programs at a sampling rate of $T_s = 0.4$ ms, which results in a velocity measurement resolution of 0.0025 m/ sec. The following control algorithms are compared:

ARC: Adaptive Robust Control - the ARC law proposed in section 4. The smooth function $S_f(\dot{q}_i)$ is chosen as $\frac{2}{\pi}\arctan(900\dot{q}_i)$. For simplicity, in the experiments, only six parameters, $\theta_1, \theta_2, \theta_5 \sim \theta_8$, are adapted. The design parameters are chosen as: $\Lambda = \mathbf{diag}[200, 30]$ and $\mathbf{K} = \mathbf{diag}[2, 1]$; $\mathbf{u_{s2}}$ is given in section 4 and $\varepsilon = 5$. The adaptation rates are set as $\Gamma = \mathbf{diag}[10, 10, 0, 0, 20, 20, 1000, 1000]$. The initial parameter estimates are chosen as: $\hat{\theta}(0) = [0.17, 0.07, 0.25, 0.27, 0.06, 0.09, 0, 0]^T$.

DCARC: Desired Compensation Adaptive Robust Control - the Desired Compensation ARC law proposed in section 5. The design parameters are chosen as: $\Lambda = \mathbf{diag}[200, 30]$, $\mathbf{K} = \mathbf{diag}[10, 1]$, $\mathbf{K_a} = \mathbf{diag}[1 \times 10^5, 1 \times 10^5]$ and $\mathbf{K_e} = \mathbf{diag}[2000, 2000]$; $\mathbf{u_{s2}}$ is given in section 5 and $\varepsilon = 1$. The adaptation rates are set as $\Gamma = \mathbf{diag}[100, 100, 0, 0, 50, 50, 1000, 1000]$. For comparison purpose, the same initial conditions as those in ARC are used.

To test the contouring performance of the proposed algorithms, the X-Y table is commanded to track a circle with radius $R = 0.1$ m at a feedrate of 314 mm/sec. The following test sets are performed:

Set 1: To test the nominal contouring performance of the controllers, experiments are run without payload, which is equivalent to $\theta_1 = 0.14$ and $\theta_2 = 0.027$;

Set 2: To test the performance robustness of the algorithms to parameter variations, a 9.1kg payload is mounted on the table, which is equivalent to $\theta_1 = 0.21$ and $\theta_2 = 0.1$;

Set 3: A large step disturbance (a simulated 0.3 V electrical signal) is added at t=0.4 sec and removed at t=1.6 sec to test the performance robustness of each controller to disturbance.

	Set 1		Set 2		Set 3	
Controller	ARC	DCARC	ARC	DCARC	ARC	DCARC
$\|\|f\|\|_{rms}$ (μm)	2.55	2.09	2.69	2.20	4.17	4.08
f_M (μm)	10.0	9.10	9.90	8.91	28.5	25.6
$\|\|u_1\|\|_{rms}$ (V)	0.18	0.20	0.19	0.19	0.23	0.23
$\|\|u_2\|\|_{rms}$ (V)	0.13	0.13	0.14	0.15	0.19	0.18
c_u	0.77	0.58	0.74	0.54	0.61	0.35

Table 1

The experimental results in terms of performance indexes are given in table 1. Overall, both ARC and DCARC achieve good contouring performance during fast movements. As seen from the table, DCARC performs better than ARC in terms of all the indexes. It also can be seen that, as expected, both controllers use almost the same amount of control effort for every test set, but ARC has a larger degree of control chattering, which agrees with the theoretical prediction stated in section 5. For Set 1, the contouring errors are given in Figure 2 which shows the nominal performance of both controllers. Tracking errors of ARC and DCARC, which are defined as $\mathbf{z} = \mathbf{q}(\mathbf{t}) - \mathbf{q_d}(\mathbf{t})$, are given in Figure 3 and 4, respectively. These two figures show that both controllers achieve good tracking accuracy, in addition to good contouring performance. The control inputs of ARC are shown in Figure 5. As seen, the input signals are within their physical limits. The control inputs of DCARC have similar shapes as those in Figure 5 and thus are not given here. For Set 2, the contouring errors are given in Figure 6. It shows that both controllers achieve good contouring performance in spite of the change of inertia load. The contouring errors for Set 3 are given in Figure 7. As seen from the figures, the added large disturbance does not affect the contouring performance much, except for the spikes when the sudden changes of the disturbance occur. This result illustrates the performance robustness of the proposed schemes.

7 Conclusions

This paper considers contour tracking control of linear-motor-driven tables in task space. An ARC controller and a DCARC controller have been developed. The proposed controllers take into account the effect of model uncertainties coming from the inertia load, friction force and external disturbances. The resulting controllers guarantee a prescribed transient performance and final tracking accuracy in general while achieving asymptotic tracking in the presence of parametric uncertainties only. Furthermore, it is shown that the DCARC scheme, in which the regressor is calculated using desired contour information only, offers several implementation advantages. Experimental results illustrate the high-performance of the proposed ARC strategies and show the advantages and drawbacks of each method.

Acknowledgment

The authors would like to thank Dr. George T.C. Chiu for his comments and valuable suggestions.

References

[1] D. M. Alter and T. C. Tsao, "Control of linear motors for machine tool feed drives: design and implementation of h_∞ optimal feedback control," *ASME J. of Dynamic systems, Measurement, and Control*, vol. 118, pp. 649–656, 1996.

[2] P. V. Braembussche, J. Swevers, H. V. Brussel, and P. Vanherck, "Accurate Tracking control of Linear Synchronous Motor Machine tool Axes," *Mechatronics*, vol. 6, no. 5, pp. 507–521, 1996.

[3] S. Komada, M. Ishida, K. Ohnishi, and T. Hori, "Disturbance Observer-Based Motion Control of Direct Drive Motors," *IEEE Transactions on Energy Conversion*, vol. 6, no. 3, pp. 553–559, 1991.

[4] G. Otten, T. Vries, J. Amerongen, A. Rankers, and E. Gaal, "Linear Motor Motion Control Using a Learning Feedforward Controller," *IEEE/ASME Transactions on Mechatronics*, vol. 2, no. 3, pp. 179–187, 1997.

[5] L. Xu and B. Yao, "Adaptive robust precision motion control of linear motors with negligible electrical dynamics: theory and experiments," in *Proc. of American Control Conference*, pp. 2583–2587, 2000.

[6] T. C. Chiu and M. Tomizuka, "Contouring control of machine tool feed drive systems: a task coordinate frame approach," in *Dynamic Systems and control 1995*, vol. 1, 1995.

[7] Y. Koren, "Cross-coupled biaxial computer control for manufacturing systems," *ASME J. Dynamical Systems, Measurement, and Control*, vol. 102, pp. 265–272, 1980.

[8] K. Srinivasan and R. Fosdick, "Multivariable analysis and controller design for coordinated multi-axial motion control," in *Proc. American Control Conference*, pp. 95–101, 1988.

[9] Y. Koren and C. C. Lo, "Variable gain cross coupling controller for contouring," *Annals of the CIRP*, vol. 40, pp. 371–374, 1991.

[10] B. Yao and M. Tomizuka, "Adaptive robust motion and force tracking control of robot manipulators in contact with compliant surfaces with unknown stiffness," *ASME J. of Dynamic Systems, Measurement, and Control*, vol. 120, no. 2, pp. 232–240, 1998.

[11] B. Yao, "High performance adaptive robust control of nonlinear systems: a general framework and new schemes," in *Proc. of IEEE Conference on Decision and Control*, pp. 2489–2494, 1997.

[12] B. Yao and L. Xu, "Adaptive robust control of linear motors for precision manufacturing," in *The 14th IFAC World Congress, Vol. A*, (Beijing), pp. 25–30, 1999.

[13] B. Armstrong-Hélouvry, P. Dupont, and C. Canudas de Wit, "A survey of models, analysis tools and compensation methods for the control of machines with friction," *Automatica*, vol. 30, no. 7, pp. 1083–1138, 1994.

[14] S. Sastry and M. Bodson, *Adaptive Control: Stability, Convergence and Robustness*. Englewood Cliffs, NJ 07632, USA: Prentice Hall, Inc., 1989.

[15] B. Yao and M. Tomizuka, "Smooth robust adaptive sliding mode control of robot manipulators with guaranteed transient performance," *Trans. of ASME, Journal of Dynamic Systems, Measurement and Control*, vol. 118, no. 4, pp. 764–775, 1996. Part of the paper also appeared in the Proc. of 1994 American Control Conference.

[16] N. Sadegh and R. Horowitz, "Stability and robustness analysis of a class of adaptive controllers for robot manipulators," *Int. J. Robotic Research*, vol. 9, no. 3, pp. 74–92, 1990.

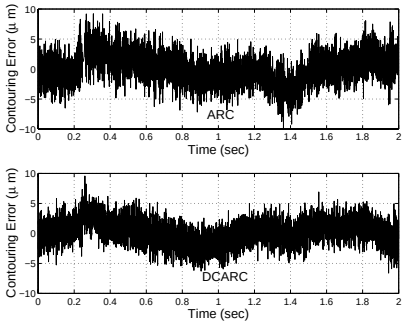

Figure 2: Contour tracking performance (without load)

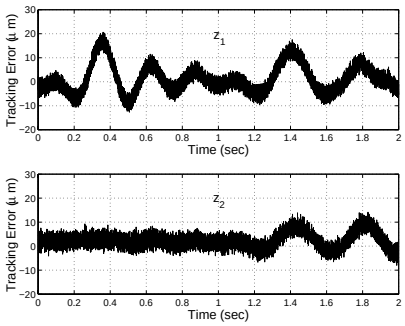

Figure 3: Tracking error of ARC (without load)

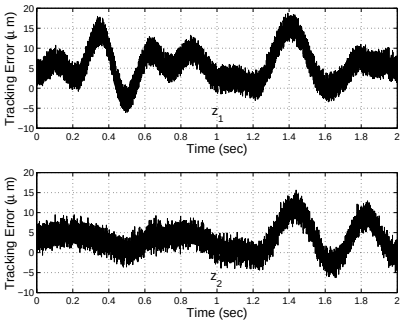

Figure 4: Tracking error of DCARC (without load)

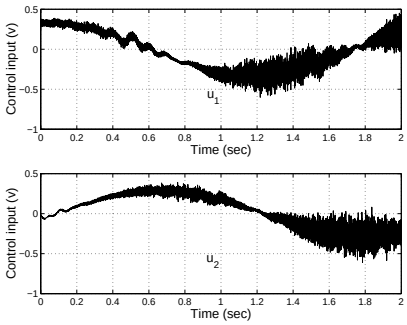

Figure 5: Control input of ARC (without load)

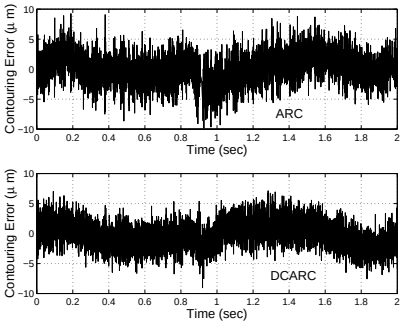

Figure 6: Contour tracking performance (with load)

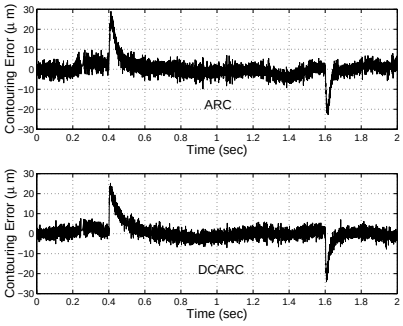

Figure 7: Contour tracking performance (with disturbance)